*Proc. Natl. Acad. Sci. USA*
Vol. 92, pp. 3673–3677, April 1995
Biochemistry

# Disruption of the adenosine deaminase gene causes hepatocellular impairment and perinatal lethality in mice

MAKI WAKAMIYA*†, MICHAEL R. BLACKBURN‡, ROLAND JURECIC*, MARK J. MCARTHUR§, ROBERT S. GESKE§, JOINER CARTWRIGHT, JR.¶, KOHNOSUKE MITANI*, SUKESHI VAISHNAV‖, JOHN W. BELMONT*, RODNEY E. KELLEMS*‡, MILTON J. FINEGOLD¶, CHARLES A. MONTGOMERY, JR.§, ALLAN BRADLEY*‖, AND C. THOMAS CASKEY*‖

Departments of *Molecular and Human Genetics and ‡Biochemistry, §Center for Comparative Medicine, ¶Department of Pathology, and ‖Howard Hughes Medical Institute, Baylor College of Medicine, Houston, TX 77030

*Contributed by C. Thomas Caskey, December 29, 1994*

**ABSTRACT** **We have generated mice with a null mutation at the *Ada* locus, which encodes the purine catabolic enzyme adenosine deaminase (ADA, EC 3.5.4.4). ADA-deficient fetuses exhibited hepatocellular impairment and died perinatally. Their lymphoid tissues were not largely affected. Accumulation of ADA substrates was detectable in ADA-deficient conceptuses as early as 12.5 days postcoitum, dramatically increasing during late *in utero* development, and is the likely cause of liver damage and fetal death. The results presented here demonstrate that ADA is important for the homeostatic maintenance of purines in mice.**

Adenosine deaminase (ADA) is a pivotal enzyme of purine catabolism. It catalyzes the irreversible deamination of adenosine (Ado) and deoxyadenosine (dAdo) to inosine (Ino) and deoxyinosine (dIno), respectively. The importance of the enzyme for vertebrate organisms stems in part from the physiological impact of its substrates. Ado functions as an extracellular signal transducer that mediates a vast array of cellular responses via interaction with cell surface receptors. Elevations in dAdo are often associated with cytotoxicity resulting from interference with deoxynucleotide metabolism (1).

In mice, the cellular localization and developmental control of ADA expression has been well studied. Prenatally, a high level of ADA expression occurs at the maternal–fetal interface, first in the secondary decidua, a maternal tissue surrounding the implanting embryo, and later in trophoblast cells of fetal origin that contribute to the formation of the chorioallantoic placenta (2). Postnatally, a very high level of ADA is found in the keratinized squamous epithelium of the upper alimentary tract (3). However, the physiological role of tissue-specific ADA is not understood.

In humans, ADA deficiency causes an autosomal recessive form of severe combined immune deficiency (1). The pathophysiology of the disease can be accounted for by the sensitivity of the lymphoid tissues to the toxic substrates. Ado, dAdo, and the metabolite dATP, which accumulate in the absence of ADA. Alternatively, ADA might be directly involved in T-cell activation, since it has been demonstrated that ADA is directly associated with human CD26, an essential accessory molecule for T-cell activation (4). These possibilities regarding the pathogenesis of ADA deficiency warrant further investigation.

In the current study, we disrupted the murine *Ada* gene in embryonic stem cells to generate ADA-deficient mice. These mice can be used as laboratory mammals for the study of tissue-specific ADA function and pathogenesis related to ADA deficiency.

The publication costs of this article were defrayed in part by page charge payment. This article must therefore be hereby marked "*advertisement*" in accordance with 18 U.S.C. §1734 solely to indicate this fact.

## MATERIALS AND METHODS

**Isolation of ADA-Targeted Embryonic Stem Cell Clones.** An 8.6-kb *Hin*dIII fragment of the murine *Ada* gene (exons 2–6) was inserted into the Bluescript II KS + vector (Stratagene). A PGKneobpA cassette (5) was inserted into a unique *Aat* II site in exon 5. Two copies of the MC1TKpA cassette (6) were inserted at the 3′ end of the homologous sequences. Culture, electroporation, and selection of AB1 embryonic stem cells (6) were as described (7). DNA was extracted from individual clones (8) and digested with the restriction enzyme *Bam*HI, and Southern blot analysis was carried out with the 3′ flanking probe (Fig. 1*A*).

**ADA and Purine Nucleoside Phosphorylase (PNP) Conversion Assay.** Crude tissue extracts were obtained by homogenizing and then freezing and thawing in 0.25 M Tris·HCl (pH 7.9). ADA activity and PNP activity were determined as described (9, 10). Each reaction mixture contained 0.8 μg of total protein.

**Histology and Electron Microscopy.** Fetuses and placentas were fixed with zinc formalin (Z-Fix, Anatech, Battle Creek, MI). The tissues were dehydrated, cleared, infiltrated, and embedded in paraffin wax. The longitudinal hemisections were cut and stained with hematoxylin/eosin. For ultrastructural studies, the liver specimens were fixed in 3% (vol/vol) glutaraldehyde, buffered with 0.1 M Pipes (pH 7.2) overnight, postfixed in 2% (wt/vol) osmium tetroxide for 1 h, dehydrated, and embedded in Spurr's resin. Sections of 60 nm were cut, stained with uranyl acetate and lead citrate, and examined in a JEOL 100C electron microscope.

**Biochemical Analysis.** Pooled plasma samples were tested for total protein, albumin, aspartate aminotransferase, and alanine aminotransferase on an automated random-access clinical chemistry analyzer (Hitachi 704, Boehringer Mannheim). To determine plasma amino acid levels, each plasma sample was analyzed individually by using a Beckman model 6300 amino acid analyzer.

**Nucleoside and Nucleotide Analysis.** Nucleosides were extracted as described (11). The HPLC system consisted of two Contrametric III pumps controlled by a GM 4000 gradient programmer, a constant wavelength UV monitor, and a CI-10B integrator (LDC Analytical, Riviera Beach, FL). Separation was through a reversed-phase Customsil ODS column (4.6 × 254 mm) with a 20-mm ODS precolumn (Custom LC, Houston). The mobile phase was 0.02 M $NH_4H_2PO_4$ (pH 5.1) with a superimposed methanol gradient. Flow rate was 1 ml/min and the injection volume was 200 μl. Absorbance was continuously monitored at a wavelength of 254 nm and peaks

Abbreviations: ADA, adenosine deaminase; PNP, purine nucleoside phosphorylase; dpc, day(s) postcoitum.

†To whom reprint requests should be addressed at: Department of Molecular and Human Genetics, Baylor College of Medicine, One Baylor Plaza, Room T832, Houston, TX 77030.

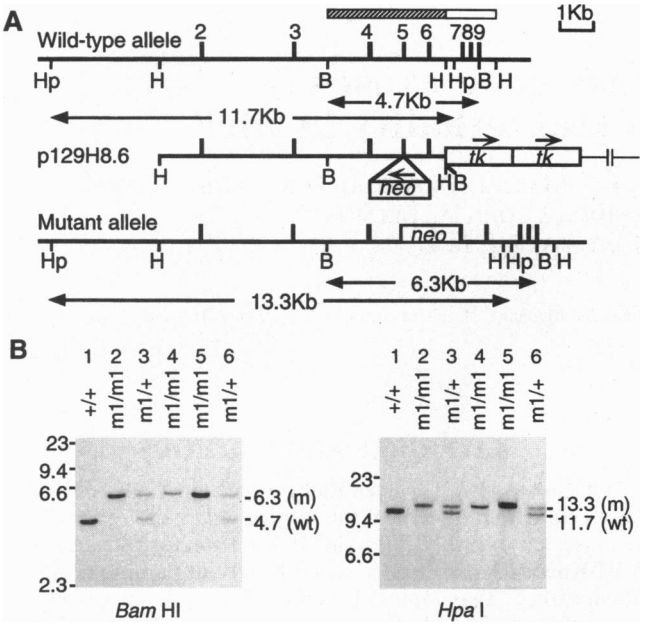


FIG. 1. Homologous recombination into the murine *Ada* locus. (*A*) Restriction enzyme maps of the murine *Ada* wild-type allele, targeting vector p129H8.6, and mutant allele. The thick line indicates genomic sequences of the murine *Ada* with exons 2–9 as thick bars. The thin line in p129H8.6 indicates plasmid vector sequences. The neomycin-resistance (neo) gene and the herpes simplex virus *tk* genes are transcribed in the direction indicated by the arrows. The hatched box indicates a 3.5-kb internal probe inside p129H8.6. The open box indicates a 1.4-kb 3′ flanking probe external to p129H8.6. H, *Hin*dIII; Hp, *Hpa* I; B, *Bam*HI. (*B*) Southern blot analysis of the murine *Ada* locus in fetuses from an $ada^{m1}/ada^{+}$ intercross. Genomic DNA (lanes 1–6) was digested with the restriction enzyme *Bam*HI or *Hpa* I and hybridized with the internal probe (*A*). Hybridizing fragments are 4.7 kb (wt, wild-type allele) and 6.3 kb (m, mutant allele) with *Bam*HI digestion and are 11.7 kb (wt) and 13.3 kb (m) with *Hpa* I digestion. The DNA size marker shown is a λ/*Hin*dIII digest and the numbers indicate kb.

were identified and quantitated based on coretention of known amounts of external standards (Sigma). Peaks of interest were verified by enzymatic shift assays. Nucleotides were extracted as described (12). HPLC conditions were the same as described above except that ion-pairing mobile phase was used with isocratic flow.

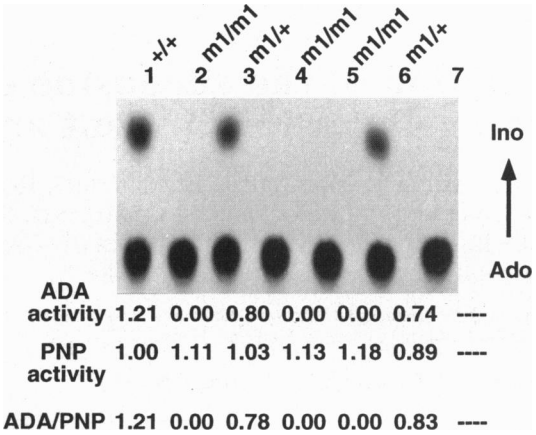


FIG. 2. ADA enzymatic activity in fetuses from an $ada^{m1}/ada^{+}$ intercross. Crude tissue extracts were prepared from 15.5-dpc fetuses (lanes 1–6). Lane 7 contains no extract. ADA and PNP activities are presented as nmol per h per μg of protein. ADA/PNP, normalized ADA activity, is a ratio of ADA activity to PNP activity.

**Flow Cytometric Analysis.** After treatment with ammonium chloride, fetal liver mononuclear cell suspensions were incubated with rat fluorescein isothiocyanate-conjugated monoclonal antibodies, specific to murine T lymphocytes (CD4, clone GK1.5; CD8, clone 53.6.7.), B lymphocytes (B220, clone RA3-6B2), granulocytes (Gr-1, clone RB6-8C5; PharMingen), and macrophages (Mac-1, clone MI/70; Boehringer Mannheim) on ice for 35 min. Flow cytometric analysis was conducted with a FACScan flow cytometer (Becton Dickinson Immunocytometry Systems) equipped with an argon ion laser (Spectra-Physics), operated at 488 nm and 300 mW. Green (fluorescein isothiocyanate) fluorescence was detected using a 530/30-nm bandpass filter. Data acquisition and analysis were performed with the FACScan LYSYS II research software (Becton Dickinson).

## RESULTS

**Generation of ADA-Deficient Mice.** A replacement-type gene targeting vector that allowed for a positive–negative selection (13) was constructed (Fig. 1*A*) and electroporated into the AB1 line of embryonic stem cells (6). The cells were then selected for resistance to G418 and 1-(2-deoxy-2-fluoro-β-D-arabinofuranosyl)-5-iodouracil. The frequency of G418-

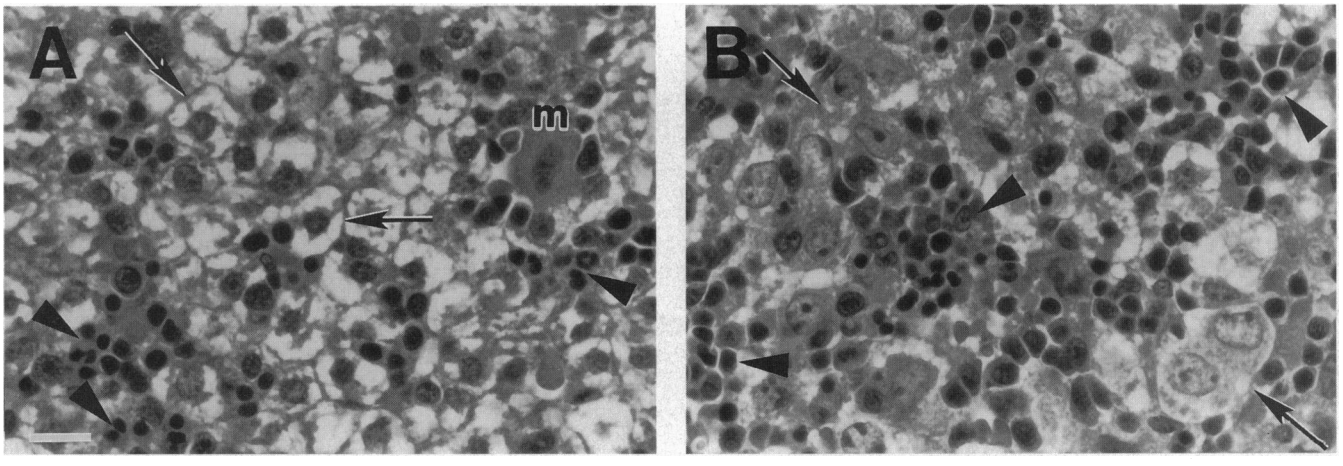


FIG. 3. Light microscopy of livers in 17.5-dpc fetuses. (*A*) Liver in $ada^{m1}/ada^{+}$ control fetus has normal-sized hepatocytes with centrally located nuclei and granular or vacuolated cytoplasm (arrows). Extramedullary hematopoiesis characterized by megakaryocytes (m) and erythrocytic or granulocytic precursor cells (arrowheads) can be seen in the hepatic sinusoids. (*B*) $ada^{m1}/ada^{m1}$ fetus with enlarged hepatocytes (arrows) and marked extramedullary hematopoiesis in sinusoids adjacent to affected hepatocytes (arrowheads). (Bar for *A* and *B* = 32 μm.)

resistant colonies was $1.9 \times 10^{-4}$ and that of double-resistant colonies was $0.2 \times 10^{-4}$ per cell electroporated. Of the 288 double-resistant colonies analyzed, 23 clones (8%) were targeted correctly. This allele is referred to as $ada^{m1}$. Of the five positive clones injected into C57BL/6J blastocysts, three clones generated chimeras that transmitted the mutation in the germ line. Heterozygous ($ada^{m1}/ada^{+}$) mice [(C57BL/6J × 129/Sv)$F_1$ hybrid] were completely viable, fertile, without abnormalities, and had ≈50% of ADA red blood cell enzymatic activity found in wild-type ($ada^{+}/ada^{+}$) mice. $ada^{m1}/ada^{+}$ mice were intercrossed to obtain homozygous ($ada^{m1}/ada^{m1}$) mutants (Fig. 1*B*).

**The $ada^{m1}$ Allele Is a Null Mutation.** ADA enzymatic activity was measured in fetuses from an $ada^{m1}/ada^{+}$ intercross (Fig. 2). A wild-type mouse converted Ado to Ino with ADA activity at 1.21 nmol per h per μg of protein. $ada^{m1}/ada^{+}$ mice had two-thirds of this activity, and none was detectable in $ada^{m1}/ada^{m1}$ mice at a level of ≤0.02 nmol per h per μg of protein. Because of a report that there may be another gene at the 3′ end of the murine *Ada* locus, we also examined this transcript by Northern blot analysis (14). We found that the transcript was not affected in the mutant fetuses (data not shown). Collectively, these studies indicate that with the insertion of the neomycin-resistance gene in exon 5, a null mutation was introduced into *Ada* but not into the downstream gene, leading to ADA-deficient mice.

**$ada^{m1}/ada^{m1}$ Mice Die Perinatally.** When $ada^{m1}/ada^{+}$ mice were intercrossed to obtain $ada^{m1}/ada^{m1}$ mice, none were found at 3 weeks of age. We observed that most of $ada^{m1}/ada^{m1}$ pups were born dead, although they were not grossly smaller or deformed compared to their littermates. Fewer than 10% of $ada^{m1}/ada^{m1}$ pups were born with beating hearts, and these did not move and remained cyanotic until they died a few hours later. Timed heterozygous matings revealed that $ada^{m1}/ada^{m1}$ fetuses were viable up to 18 days postcoitum (dpc) *in utero*, and the survival rate decreased rapidly after this time. It was found that ≈90% of $ada^{m1}/ada^{m1}$ fetuses had died by 19 dpc. The complete penetrance of $ada^{m1}/ada^{m1}$ lethality was observed in all three mutant lines generated, suggesting that disruption of the *Ada* gene alone accounted for the lethality.

**ADA-Deficient Fetuses Exhibit Hepatocellular Impairment.** Gross evidence of hepatic necrosis was observed in ADA-deficient fetuses at 17.5 dpc. Body weight and liver weight/body weight ratios of $ada^{m1}/ada^{m1}$ fetuses were decreased by 15% and 29%, respectively, at late gestation. Liver function tests performed in pooled plasma samples from 17.5-dpc fetuses showed that $ada^{m1}/ada^{m1}$ fetuses had hypoproteinemia (59% reduction) and hypoalbuminemia (57% reduction), whereas there were no significant changes in plasma amino acids, which are readily supplied to fetuses by the maternal circulation. $ada^{m1}/ada^{m1}$ fetuses also had elevated levels of two hepatocellular enzymes, aspartate aminotransferase (66% elevation) and alanine aminotransferase (56% elevation). These findings are all compatible with hepatocellular dysfunction, necrosis, and leakage.

Histological analysis was performed on fetuses ranging from 12.5 dpc to 18.5 dpc and on 17.5-dpc placentas. In $ada^{m1}/ada^{m1}$ fetuses, liver was the only organ that was identified as abnormal. No morphologic lesions were detected in any major lymphoid organs, including thymus, spleen, gut-associated lymphoid tissues, and bronchial-associated lymphoid tissue, nor were any other lesions reported in ADA-deficient humans detected (15, 16). $ada^{m1}/ada^{+}$ fetuses had normal livers (Fig. 3*A*). In contrast, the livers from $ada^{m1}/ada^{m1}$ fetuses contained hepatic plates that were disorganized, resulting in isolated packets of cells (Fig. 3*B*). There was a quantitative decrease in numbers of hepatocytes per lobule, and the hepatocytes illustrated a variety of morphological changes that were consistent with hepatocellular impairment. The morphologic changes in $ada^{m1}/ada^{m1}$ hepatocytes were detectable in some cells as early as 16.5 dpc and the number of affected cells increased with gestational age. At 18.5 dpc, hepatocellular degeneration and necrosis were widespread.

Ultrastructural examination illustrated enlarged hepatocytes with karyomegaly, irregularly shaped nuclear envelopes, and a significant decrease in heterochromatin in $ada^{m1}/ada^{m1}$ livers. A single large nucleolus was often observed. The cytoplasm of affected cells had decreased amounts of glycogen, normal mitochondria, and an increased volume of rough endoplasmic reticulum. Hepatocytes lost their normal polyhedral shape and became round, and individual cells were in close apposition to each other (Fig. 4).

**ADA Substrates and dATP Are Markedly Elevated in $ada^{m1}/ada^{m1}$ Mice.** To investigate the biochemical consequences of ADA deficiency, purine nucleoside concentrations were examined in fetuses and placentas at 10.5 dpc through 17.5 dpc by using reversed-phase HPLC. Ado concentrations were elevated in $ada^{m1}/ada^{m1}$ fetuses at all stages and increased with development (Fig. 5*A*). dAdo was not detected in $ada^{+}/ada^{+}$ or $ada^{m1}/ada^{+}$ fetuses at any stage examined, but

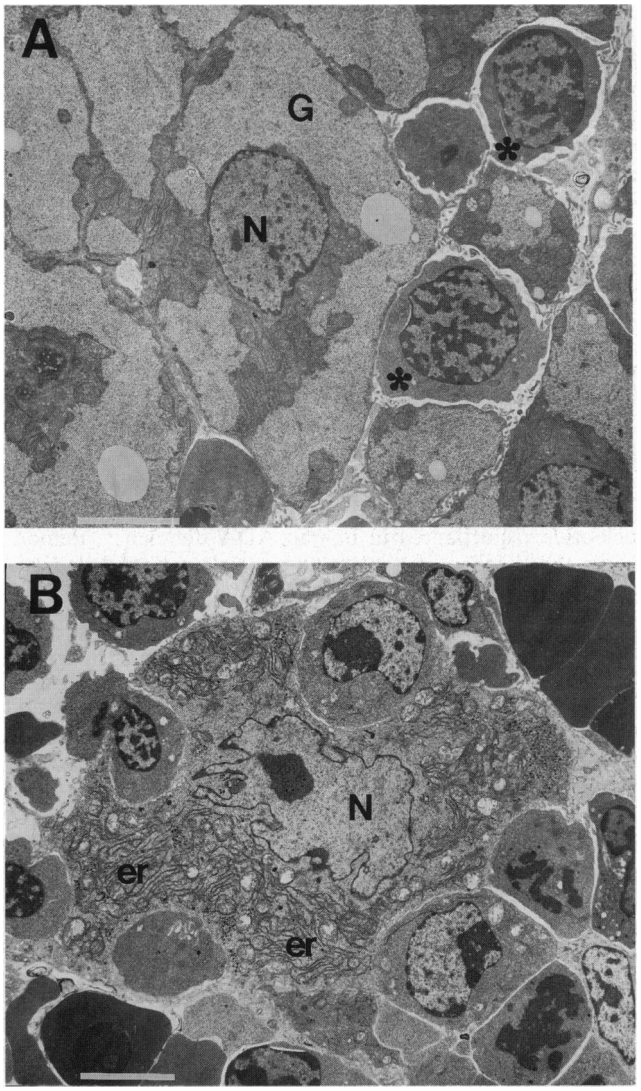


FIG. 4. Electron microscopy of livers in 17.5-dpc fetuses. (*A*) Liver in $ada^{m1}/ada^{+}$ control fetus with angular shaped hepatocytes, abundant cytoplasmic glycogen (G), and an oval nucleus (N) with evenly distributed heterochromatin. Erythrocytic precursor cells (*) are adjacent to hepatocytes. (*B*) Enlarged hepatocyte from $ada^{m1}/ada^{m1}$ fetus has increased amounts of cytoplasmic rough endoplasmic reticulum (er) and an irregular shaped nucleus (N) with infolding of the nuclear envelope. (Bars: A, 2 μm; B, 5 μm.)

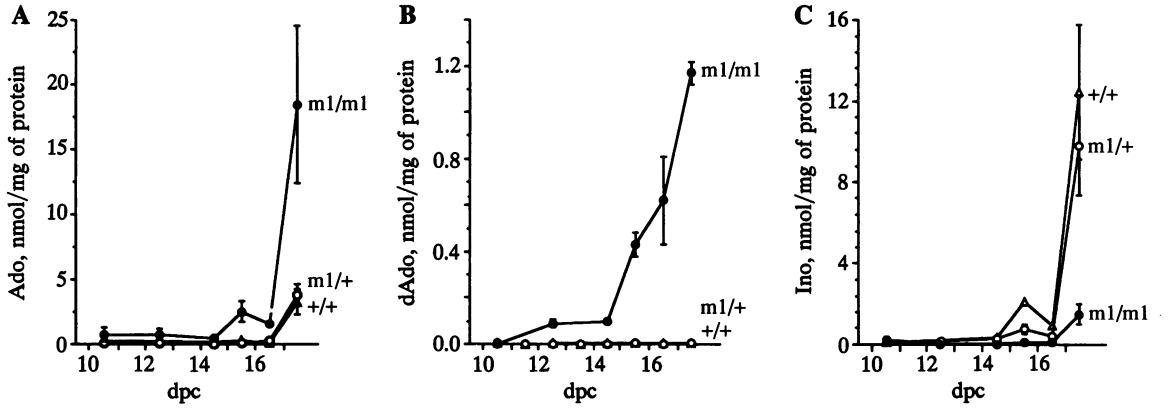


FIG. 5. Ontogeny of nucleosides in fetuses from $ada^{m1}/ada^{+}$ intercrosses. Nucleoside concentrations are presented as nmol/mg of protein (mean ± SEM). The numbers of conceptuses examined were on average 3 $ada^{+}/ada^{+}$, 7 $ada^{m1}/ada^{+}$, and 4 $ada^{m1}/ada^{m1}$ at 10.5, 12.5, 14.5, 15.5, 16.5, and 17.5 dpc. (*A*) Fetal adenosine levels. (*B*) Fetal deoxyadenosine levels. (*C*) Fetal inosine levels.

increased in $ada^{m1}/ada^{m1}$ fetuses during development so that by 17.5 dpc, dAdo concentrations were 1.17 nmol/mg of protein, at least 1000-fold higher than levels found in wild-type fetuses (Fig. 5*B*). Ino levels increased in $ada^{+}/ada^{+}$ fetuses during late fetal development but remained low throughout development in $ada^{m1}/ada^{m1}$ fetuses (Fig. 5*C*). dIno levels were below the level of detection in fetuses irrespective of genotype. The $ada^{m1}/ada^{m1}$ placentas, which normally express high levels of ADA, exhibited similar patterns in changes of Ado and Ino concentrations during gestation as seen in the fetuses, but accumulation of dAdo was not observed (data not shown).

Adenine nucleotide levels were also examined in blood from 17.5-dpc fetuses to monitor alterations in deoxynucleotide metabolism (Table 1). The dATP levels in $ada^{m1}/ada^{m1}$ fetal blood was elevated by 2000-fold, while ATP levels decreased slightly. Thus, these data indicate that adenine nucleoside catabolism is profoundly affected in ADA-deficient conceptuses and accumulated dAdo may be phosphorylated to dATP. The ratio of dATP to ATP, which is often used for analysis of nucleotide disturbances in human ADA deficiency, demonstrates the severity of nucleotide pool alterations in $ada^{m1}/ada^{m1}$ fetuses.

**Hematopoietic Cells in $ada^{m1}/ada^{m1}$ Mice.** To evaluate leukocyte subpopulations in $ada^{m1}/ada^{m1}$ fetuses, flow cytometric analysis with the cell surface markers CD4, CD8, B220, Gr-1, and Mac-1 was carried out on livers of 14.5-dpc and 16.5-dpc fetuses (Table 2). T cells, B cells, granulocytes, and macrophages were found in substantial amounts in the fetuses examined, regardless of the genotype. The two-sample *t* test revealed that the percentages of $CD4^{+}$ cells and $CD8^{+}$ cells in $ada^{m1}/ada^{m1}$ mice were significantly different from those of age-matched controls at 16.5 dpc ($0.02 < P < 0.05$). Thus, mature T-cell subpopulations in $ada^{m1}/ada^{m1}$ mice were decreased compared to controls at 16.5 dpc, although the decrease was not as dramatic as the lymphocyte depletion seen in human ADA-deficient patients.

Table 1. ATP and dATP concentrations in 17.5-dpc fetal blood

| Fetus | ATP, nmol/mg of protein | dATP, nmol/mg of protein | dATP/ATP | *n* |
|---|---|---|---|---|
| $ada^{+}/ada^{+}$ | 10.8 | ND* | – | 1 |
| $ada^{m1}/ada^{+}$ | 13.3 ± 2.8 | 0.4 ± 0.3 | 0.03 | 5 |
| $ada^{m1}/ada^{m1}$ | 6.0 ± 0.1 | 2.4 ± 0.2 | 0.40 | 2 |

Values are the mean ± SEM.
*ND, not detected at a level of ≤0.001 nmol/mg of protein.

## DISCUSSION

Changes in the relative concentrations of ADA substrates in $ada^{m1}/ada^{m1}$ conceptuses during late *in utero* development were dramatic, which suggests that under normal conditions there is a considerable flux of adenine nucleosides through the ADA-catalyzed reaction. The metabolic load of ADA substrates in fetuses was so great that the maternal circulatory system could not adequately reduce these nucleosides to nontoxic levels, probably due to a slower rate of nucleoside passage across the placental barrier compared to the rate of production and input of nucleosides to the fetuses. A variety of cytotoxic effects caused by Ado, dAdo, and particularly dATP are believed to contribute to the pathogenesis of human ADA deficiency, and it is likely that the liver pathology found in $ada^{m1}/ada^{m1}$ mice is also associated with the accumulation of these molecules. In mice, the major pathway of dAdo phosphorylation is thought to be through the enzyme adenosine kinase, which is fairly abundant in liver (17, 18), and the highest levels of dAdo phosphorylation activity are found in the liver of adult mice (18). Therefore, it is possible that dATP selectively accumulates in the liver of $ada^{m1}/ada^{m1}$ fetuses to cause selective impairment of this organ. Investigating tissue-specific accumulations of dATP in $ada^{m1}/ada^{m1}$ fetal livers should clarify this matter. Adult liver is also a site of synthesis of the enzyme *S*-adenosylhomocysteine hydrolase, whose inhibition by dAdo should be considered as a possible mechanism of the liver degeneration seen in $ada^{m1}/ada^{m1}$ fetuses (19). It has recently been reported (20) that lack of this enzyme can lead to early embryonic lethality in mice. Determining levels of the *S*-adenosylhomocysteine hydrolase activity in the mutants will be necessary to test this possibility.

The ADA-deficient phenotype in mice differs some from that of humans, a result observed in other purine metabolism deficiencies in mice such as hypoxanthine-guanine phosphoribosyltransferase deficiency and uricase deficiency (7, 21). Accumulation of toxic metabolites, and the subsequent lymphopenia and developmental arrest in the thymus, can be detected in human ADA-deficient fetuses as early as the second trimester (22) and the patients die of overwhelming infection accompanying severe combined immunodeficiency. However, it is unlikely that $ada^{m1}/ada^{m1}$ mice have severe combined immunodeficiency, since their lymphoid tissues were histologically normal at 17.5 dpc. Furthermore, we did not find any evidence of infection. Because of the potential importance of fetal hepatic function and the sequence of the events in $ada^{m1}/ada^{m1}$ fetuses before fetal death (first a purine metabolism anomaly, moderate-to-progressive hepatocellular degeneration, and then cell death), it is likely that liver disease due to purine metabolic disturbances is responsible for the

Table 2. Flow cytometric analysis of leukocyte subpopulation in fetal liver

| Age, dpc | Genotype | *n* | % of total cells | | | | |
|---|---|---|---|---|---|---|---|
| | | | CD4 | CD8 | B220 | Gr-1 | Mac-1 |
| 14.5 | +/+ and m1/+ | 10 | 2.05 ± 0.75 | 3.16 ± 0.96 | 6.05 ± 1.65 | 2.19 ± 0.51 | 0.38 ± 0.28 |
| | m1/m1 | 3 | 3.00 ± 0.78 | 4.13 ± 1.66 | 8.34 ± 4.86 | 3.84 ± 2.84 | 0.63 ± 0.49 |
| 16.5 | +/+ and m1/+ | 9 | 2.37 ± 0.47* | 2.99 ± 0.60* | 5.46 ± 1.18 | 2.08 ± 0.53 | 0.38 ± 0.32 |
| | m1/m1 | 6 | 1.63 ± 0.62* | 2.26 ± 0.61* | 4.74 ± 1.02 | 1.95 ± 1.36 | 0.22 ± 0.22 |

Values are the mean ± SD.
*Significantly different between $ada^{m1}/ada^{m1}$ and the control ($0.02 < P < 0.05$ in two-sample *t* test).

lethality. However, further examination of the immunological status and the possibility of congenital infection in $ada^{m1}/ada^{m1}$ mice should be performed.

ADA is highly expressed at the maternal–fetal interface throughout postimplantation development, first on the maternal side (decidua) and later in the fetal placenta (2). Profound changes in purine catabolism in $ada^{m1}/ada^{m1}$ fetuses became evident at ≈14.5 dpc, when decidual ADA was coincidentally lost, indicating a possible involvement of decidual ADA in purine metabolism during early postimplantation stage of development. It is possible that decidual ADA prevents the accumulation of some toxic substrates during early postimplantation stages of development (11). Placental ADA may have a similar responsibility during the remainder of development. The results presented here demonstrate the metabolic importance of ADA in mammalian organisms and have exposed the vital function of murine embryonic ADA. Our ADA-deficient mice will be useful as laboratory mammals for the study of tissue-specific ADA function and pathogenesis related to ADA deficiency. In addition, it might be possible to rescue $ada^{m1}/ada^{m1}$ mice by gene transfer techniques using recombinant adenoviruses or liposomes. Another possibility could be rescue by genetic reconstitution of placenta-specific ADA expression in ADA-deficient mice by using placenta-specific regulatory elements characterized in the murine *Ada* gene (23). Such approaches could enhance the utility of these ADA-deficient mice as an animal model.

We thank Dr. R. R. Behringer for the mouse genomic DNA library, Dr. F. Rudolph for the use of his HPLC system, Dr. N. T. Van for the use of the FACScan system, and L. McGuffey, A. W. Warman, S. E. Robbins, M. Hsiao, I. M. Upton, D. J. Burton, and M. Coolbaugh-Murphy for technical assistance. We thank Drs. W. E. O'Brien, R. Ramírez-Solis, A. C. Davis, M. Wims, J. D. Wallace, J. H. Winston, and X. Wu for valuable technical guidance. We also thank Dr. B. J. F. Rossiter for critical review of the manuscript. This work was supported by grants from National Institute of Diabetes and Digestive and Kidney Diseases (5R01DK42696 and 5R01DK46207), National Heart, Lung, and Blood Institute (1R01HL51232), and National Institute of Child Health and Human Development (1R01HD30302). C.T.C. and A.B. are investigators with the Howard Hughes Medical Institute. M.R.B. was supported by a National Institutes of Health postdoctoral fellowship (1F32HD07843-01).

1. Kredich, N. M. & Hershfield, M. S. (1989) in *Immunodeficiency Diseases Caused by Adenosine Deaminase Deficiency and Purine Nucleoside Phosphorylase Deficiency*, eds. Scriver, C. R., Beaudet, A. L., Sly, W. S. & Valle, D. M. (McGraw–Hill, New York), pp. 1045–1075.
2. Knudsen, T. B., Blackburn, M. R., Chinsky, J. M., Airhart, M. J. & Kellems, R. E. (1991) *Biol. Reprod.* **44,** 171–184.
3. Chinsky, J. M., Ramamurthy, V., Fanslow, W. C., Ingolia, D. E., Blackburn, M. R., Shaffer, K. T., Higley, H. R., Trentin, J. J., Rudolph, F. B., Knudsen, T. B. & Kellems, R. E. (1990) *Differentiation* **42,** 172–183.
4. Kameoka, J., Tanaka, T., Nojima, Y., Schlossman, S. F. & Morimoto, C. (1993) *Science* **261,** 466–469.
5. Soriano, P., Montgomery, C., Geske, R. & Bradley, A. (1991) *Cell* **64,** 693–702.
6. McMahon, A. P. & Bradley, A. (1990) *Cell* **62,** 1073–1085.
7. Wu, X., Wakamiya, M., Vaishnav, S., Geske, R., Montgomery, C., Jr., Jones, P., Bradley, A. & Caskey, C. T. (1994) *Proc. Natl. Acad. Sci. USA* **91,** 742–746.
8. Ramírez-Solis, R., Rivera-Pérez, J., Wallace, J. D., Wims, M., Zheng, H. & Bradley, A. (1992) *Anal. Biochem.* **201,** 331–335.
9. Van der Weyden, M. B. & Bailey, L. (1978) *Clin. Chem. Acta* **82,** 179–184.
10. Aitken, D. A., Kleijer, W. J., Niermeijer, M. F., Herb-Schleb-Voogt, E. & Galjaard, H. (1980) *Clin. Genet.* **17,** 293–298.
11. Knudsen, T. B., Winters, R. S., Otey, S. K., Blackburn, M. R., Airhart, M. J., Church, J. K. & Skalko, R. G. (1992) *Teratology* **45,** 91–103.
12. Gao, X., Blackburn, M. R. & Knudsen, T. B. (1994) *Teratology* **49,** 1–12.
13. Thomas, K. R. & Capecchi, M. R. (1987) *Cell* **51,** 503–512.
14. Al-Ubaidi, M. R., Ramamurthy, V., Maa, M.-C., Ingolia, D. E., Chinsky, J. M., Martin, B. D. & Kellems, R. E. (1990) *Genomics* **7,** 475–485.
15. Ratech, H., Hirschhorn, R. & Greco, M. A. (1989) *Am. J. Pathol.* **135,** 1145–1156.
16. Ratech, H., Gallo, G., Rimoin, D. L., Kamino, H. & Hirschhorn, R. (1985) *Am. J. Pathol.* **120,** 157–169.
17. Ullman, B., Gudas, L. J., Cohen, A. & Martin, D. W. (1978) *Cell* **14,** 365–375.
18. Carson, D. A., Kaye, J. & Wasson, D. B. (1980) *J. Immunol.* **124,** 8–12.
19. Hershfield, M. S. (1979) *J. Biol. Chem.* **254,** 22–25.
20. Miller, M. W., Duhl, D. M. J., Winkes, B. M., Arredondo-Vega, F., Saxon, P. J., Wolff, G. L., Epstein, C. J., Hershfield, M. S. & Barsh, G. S. (1994) *EMBO J.* **13,** 1806–1816.
21. Kuehn, M. R., Bradley, A., Robertson, E. J. & Evans, M. J. (1987) *Nature (London)* **326,** 295–298.
22. Linch, D. C., Levinsky, R. J., Rodeck, C. H., MacLennan, K. A. & Simmonds, H. A. (1984) *Clin. Exp. Immunol.* **56,** 223–232.
23. Winston, J. H., Hanten, P. A., Overbeek, P. A. & Kellems, R. E. (1992) *J. Biol. Chem.* **267,** 13472–13479.